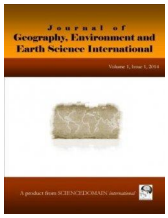

Journal of Geography, Environment and Earth Science International

15(1): 1-12, 2018; Article no.JGEESI.41461
ISSN: 2454-7352

Mapping of Geomorphological Features and Surface Sediments in Nekhel Area, Sinai Peninsula, Egypt Using Integration between Full-polarimetric SAR (RADARSAT-2) and Optical Remote Sensing Data

Islam Abou El-Magd[1*], Hassan Mohy[2] and Ali Amasha[3]

[1]Department of Environmental Studies, National Authority for Remote Sensing and Space Sciences, Cairo, Egypt.
[2]Department of Geology, Cairo University, Egypt.
[3]Arab Academy for Science, Technology and Maritime Transport, Egypt.

Authors' contributions

This work was carried out in collaboration between all authors. Author IAEM designed the research study, shared in the analysis of the data, writing the manuscript and managed the submission to the journal. Authors HM and AA shared in the analysis of the data, managed the literature searches and shared writing the manuscript. All authors read and approved the final manuscript.

Article Information

DOI: 10.9734/JGEESI/2018/41461
Editor(s):
(1) Wen-Cheng Liu, Department of Civil and Disaster Prevention Engineering, National United University, Taiwan and Taiwan Typhoon and Flood Research Institute, National United University, Taipei, Taiwan.
Reviewers:
(1) Işın Onur, Akdeniz University, Turkey.
(2) M. I. M Kaleel, South Eastern University of Sri Lanka, Sri Lanka.
Complete Peer review History: http://www.sciencedomain.org/review-history/24532

Original Research Article

Received 21st February 2018
Accepted 1st May 2018
Published 8th May 2018

ABSTRACT

Key element for developing countries in remote sensing research is the availability of data particularly the newly developed sensors such as SAR data. This research aims at exploring the potentiality of utilising RADARSAT-2 (which is obtained freely from Canadian Space Agency) in integration with optical data from Landsat 8 and ASTER sensors for lithological mapping of the Nekhel area, Sinai Peninsula, Egypt. Optical enhancements such as Principal Component Analysis together with Spectral rationing of selected bands of Landsat 8 and ASTER data provided an active approach in characterising the surface sediments and mapping the lithology of the area of study. Data fusion of optical and radar remote sensing data using Color Normalization Transformation

**Corresponding author: E-mail: imagd@narss.sci.eg;*

aided for further characterization and improvement of identification of lithological units. The Freeman-Durden decomposition method used to determine the dominant scattering mechanisms and to outline the current state of the surface cover. Mapping and characterising surface sediment of desert environments regarding their spectral and backscattering characteristics provide essential information on the geomorphology and depositional history to assess their potential use for economic development.

Keywords: RADARSAT-2; optical; ASTER; Landsat 8; Lithological mapping; sediment; Sinai.

1. INTRODUCTION

Peninsula of Sinai is a triangular-shaped region covering 61,000 km^2 between North Africa and West Asia, which is geologically controlled with major structures. A significant portion of the Northern and Middle part of Sinai is covered with sediments. It is important to characterize the desert surface sediments and their spatial distribution regarding surface roughness that can reveal information about the depositional history and environment as well as active surface processes [1,2]. Remotely sensed data had been widely used in the mapping of Land Use and Land Cove, monitoring of crops and its condition, mapping the geomorphology and geological structures as well as geo-environmental hazards studies. The primary source of remotely sensed data is the optical data (which is dependent on sunlight) sometimes due to unfavorable weather conditions is not always appropriate. Therefore, Synthetic Aperture Radar (SAR) sensors, such as the one onboard RADARSAT-2, are able to transmit microwaves through cloud cover, rain and aerosol-polluted skies; thus offering an alternative data source favorable for all weather conditions and independent of sunlight.

SAR sensors always measure the amount of backscattered energy, which is affected by two different parameters, namely the surface roughness (represented by the root mean square height) and the complex dielectric constant (ϵ) of the earth surface cover. SAR data always rely on the quantitative energy either 1) the permittivity, which determines the portion of energy that penetrates the material and the rest of the energy is scattered off the surface; or 2) electrical conductivity, which determines the portion of the energy that is lost as heat or scattering inside the material.

It is commonly known that high permittivity means less penetration of energy (hence more reflection/scattering at the surface), while high loss means more energy dissipation inside the material. The property of the object always reflected on the quantity of energy either penetrated or scattered, therefore, increasing bubble contents of the sedimentary soil means more penetration and therefore higher volume scattering and higher measured backscatter. Alternatively, high moisture contents means higher conductivity, higher loss, and therefore less backscatter.

Single polarized SAR data provides a single value of reflectivity for each pixel in a scene, whereas full-polarimetric SAR data provides additional information such as the dependence of reflectivity on polarization for each pixel in the scene by measuring both the intensity of the backscattered waves and changes in its polarization and phase (ϕ) [3]. The signature of radar signals for specific target permits stronger impacts of the physical scattering mechanism than single polarization measurements through identification and characterization of the dominant scattering mechanism. Therefore, it could be resolved based on the geometric shape and dielectric constant of the object [4]. This create more potentiality of the radar polarimetry imaging for soil and surface sediments discrimination in terms of surface roughness, grain size, volumetric moisture content and heterogeneity [5,6,7].

More importantly and different from optical sensors radar data are sensitive to surface roughness, moisture contents, porosity and morphology. On the other hand, optical multi-spectral remote sensing data provides characterization of the surface objects based on their optical properties in the specific wavelength. Hence, the integration between both datasets might create further potentials in the analysis and obtain more information that might not obtain from a single source. This is the main objective of this research is to demonstrate the effectiveness of integrating both optical and SAR remote sensing data to map and characterize the lithology and surface sediments in portion of central Sinai.

2. AREA OF STUDY

The area of study is part of Sinai Peninsula, Egypt, which is located nearly 115 km east of Suez city, 90 km west of Taba town (Fig. 1). The area of study is bounded by latitudes 29° 35' and 29° 55' N and longitudes 33° 40' and 34° 05' E. The dominant climatic condition of the area is arid.

3. DATA AND METHODS

3.1 Data

3.1.1 The optical remote sensing data (Landsat 8 and ASTER)

In this research two main optical multispectral data sensors were used, which are Landsat 8 and ASTER. Landsat 8 spectral bands has 11 channels that cover wide range of the electromagnetic radiation including visible and the near infrared (VNIR), shortwave infrared (SWIR) and thermal infrared range (TIR).The spatial resolution varies from 30 m for VNIR and SWIR (channels 1-7 and 9), 15 m for the panchromatic band 8, to 100 m for TIR (channel 10 and 11).

The Advanced Space borne Thermal Emission and Reflection Radiometer (ASTER) includes14 channels, that cover the following range of electromagnetic radiation:

- 3 channels cover the visible and near-infrared (VNIR) spectrum with 15 m spatial resolution,
- 6 channels cover the short-wave infrared (SWIR) spectrum with 30 m spatial resolution, and
- 5 channels cover the thermal infrared (TIR) with 90 m spatial resolution.

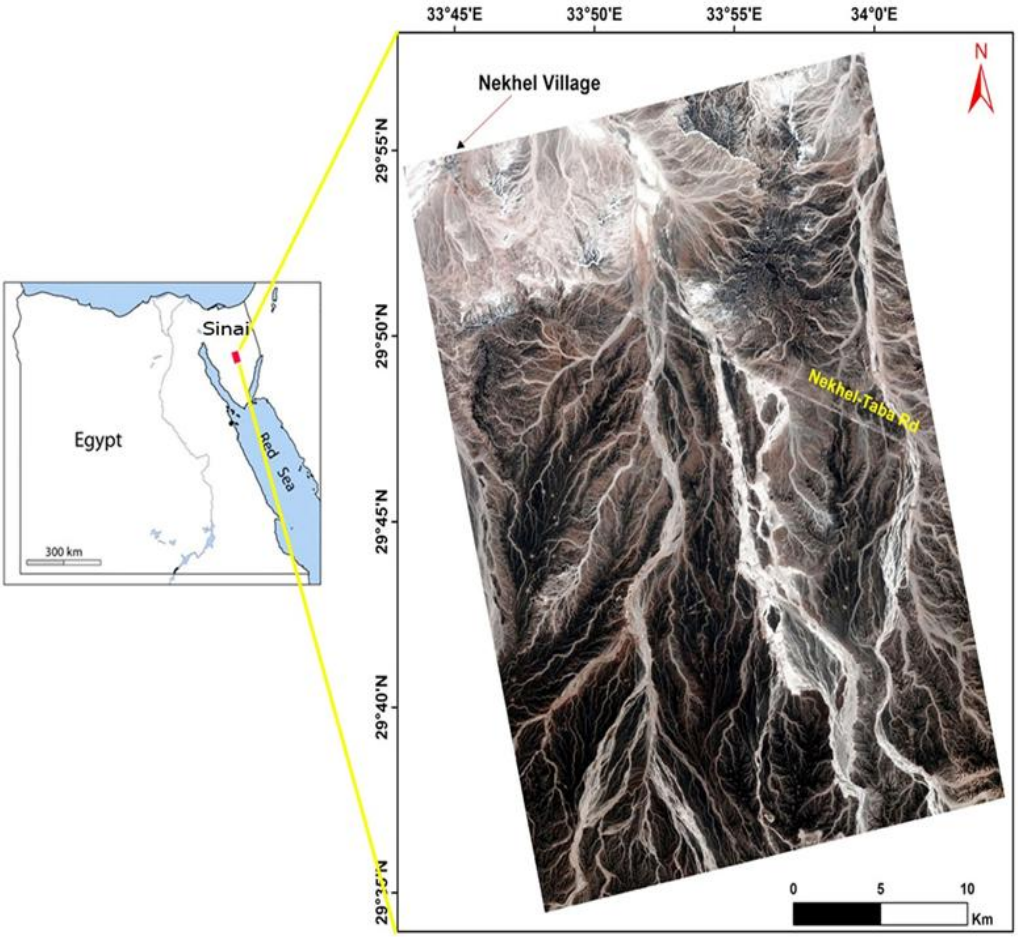

Fig. 1. Location map of the Nekhel area of study, Sinai Peninsula

Unique combination of extensive spectral coverage and high spatial resolution in the visible and near-infrared through short-wave infrared to the thermal infrared regions are an advantage of ASTER data.

3.1.2 Radar remote sensing data (RADARSAT-2)

The second main component of the data sources is the RADARSAT-2. RADARSAT-2 satellite was initially developed to improve the SAR systems' applications in sea ice mapping and iceberg detection. It is further shown high importance in marine surveillance for ships and pollution detection, geological mapping, wetlands mapping, and agricultural crop monitoring [8].

It is necessary to promote this technology in developing countries and extend its applications for societal benefits. Therefore, throughout the cooperation with the Canadian Space Agency, the data is disseminated for further usage and applications in developing countries. RADARSAT-2 offers fully polarimetric (HH, HV, VH, VV) radar imagery as well as multiple other beam modes, resolutions and incidence angles. RADARSAT-2 operates in the C-band (5.405 GHz) with a wavelength of 5.55 cm.

The satellite is in a polar sun-synchronous orbit at an altitude of approximately 798 km. The orbit has a period of 101 minutes and allows for a 24-day ground repeat. Due to its ability to acquire images at different incidence angles, it is possible to image the same area more than once in a 24 day repeat period. RADARSAT-2 uses horizontal and vertical polarizations sending alternating pulses of each. RADARSAT-2 has two receivers and so can receive both horizontal and vertical polarisations simultaneously. Data was delivered as Single-Look Complex (SLC) data. The image was acquired in standard quad-polarised (SQ4) mode on September 25, 2013. The incidence angles varied from 22.2° to 24.11° and the orbit (Ascending). Table 1 presents principal characteristics of the RADARSAT-2 data in the standard quad beam mode.

3.2 Methods

The optical remotely sensed data (Landsat 8 and ASTER) were atmospherically corrected and geometrically corrected before starting an analysis. Various image processing techniques were used to analyze both Landsat 8 and ASTER data including band combination, Principal Component Analysis (PCA) and band rationing. False colour composite (RGB) is capable of differentiating between some surface materials based on colour variation and the object behave with the optical wavelength. Principal Component Analysis (PCA) is a statistical analysis that used to produce uncorrelated bands as well as to reduce noise and the dimensionality of massive datasets. Alternatively, band rationing is a digital image processing technique that map algebra different bands in different wavelengths to effectively categories the variation in the spectral response of the geomorphological units and surface sediments [9,10]. This method is frequently used to reduce the variable effects of solar illumination and topography and enhance spectral information in the image [11].

Table 1. Overview of the principal characteristics of the RADARSAT-2 data in the standard quad beam mode

Band	C-band
Frequency	5.405 GHz
Polarisation	HH, HV, VV, VH
Approximate Resolution [range × azimuth] m^2	25 × 28
Nominal swath width (km)	25
Nominal Incidence Angle Range [deg]	18 - 49
Altitude (average)	798 km
Inclination	98.6 degrees
Period	100.7 minutes
Ascending node	18:00 hrs
Sun-synchronous	14 orbits per day
Repeat cycle	24 days

The recent advancement in remote sensing technology and image processing techniques particular in data integration (data fusion and data merging) has become an efficient tool for discrimination and visualization of the data. This is a process whereby data with different spatial and spectral characteristics over the same region are processed and evaluated in a single Red–Green–Blue (RGB) colour combination image. The Color Normalization Transformation (CNT) technique [12] is used to fuse Landsat 8 and ASTER data with RADARSAT-2 data. Conventionally, remote sensing data fusion techniques have been used to improve the spatial resolution of optical multi-spectral remote sensing data by combining these with panchromatic grayscale images with better spatial resolution [13,14]. However, in this study, the grayscale RADARSAT-2 image (T33) has been used together with optical multi-spectral remote sensing Landsat 8 and ASTER to display spectral, back-scattering and volume-scattering variations of the terrain in a single RGB colour combination image. The algorithm for CNT can be summarized as follows:

$$DN_{R(CNT)} = \frac{(DN_R)\,(DN_{radar})}{DN_R + DN_G + DN_B}$$

$$DN_{G(CNT)} = \frac{(DN_G)\,(DN_{radar})}{DN_R + DN_G + DN_B}$$

$$DN_{B(CNT)} = \frac{(DN_B)\,(DN_{radar})}{DN_R + DN_G + DN_B}$$

Where DN_R, DN_G, and DN_B are the DN values of individual pixels of the optical multi-spectral bands (Landsat 8 - ASTER) used in the RGB colour combination images. DN_{radar} is the DN values of individual pixels of the grayscale RADARSAT-2 image (T33). $DN_{R(CNT)}$, $DN_{G(CNT)}$ and $DN_{B(CNT)}$ are the DN values of the corresponding pixels of bands used in the RGB colour combination image after CNT.

Polarimetric SAR is a technology that exploits the polarized nature of electromagnetic waves to extrapolate multi-dimensional information from imaged targets [4]. The polarisation of a wave is the description of the spatial orientation of the electric vector for a given wave [15]. In a polarised transmitted signal, the electric field of SAR data is either H- or V-polarized. The scattering coefficient is measured for thousands of points in the scene. In fully polarimetric SARs the polarisation of the backscattered wave is measured as a vector quantity identified by the transmitted polarization and the receive polarization [4]. Fully polarimetric SAR data provides the 2 × 2 target scattering matrix, also referred to as the Sinclair scattering matrix:

$$S = \begin{bmatrix} S_{HH} & S_{HV} \\ S_{VH} & S_{VV} \end{bmatrix}$$

Knowledge of the scattering matrix permits calculation of the received power for any combination of transmits and receives antennas and is referred to as polarization synthesis [6]. In this work, the quad polarization from RADARSAT-2 was used to classify the surficial sediments of the study area based on the energy and scattering mechanism (degree of randomness) of radar signals that will be scattered back from different soil characteristics. Each quad polarization image was extracted using PolSARpro open source software and transformed from (2 × 2) Sinclair Matrix into (3 × 3) complex Coherence matrix [T3]. The (3 × 3) Coherency matrix [T3] is constructed from a three-element unitary target vector, obtained from the projection of a Sinclair matrix onto a reduced and modified Pauli spin matrix set [16]. It is an incoherent polarimetric representation relating to second order statistics of scattering matrix elements. This matrix is hermitian semi-definite positive [17]:

$$[T_3] = \begin{bmatrix} T_{11} & T_{12} & T_{13} \\ T_{12} & T_{22} & T_{23} \\ T_{13} & T_{23} & T_{33} \end{bmatrix}$$

The [T3] matrix of each quad SAR scene was imported into NEST ESASAR tool box and its new metadata files were replaced with the corresponding metadata files of the original raw quad SAR data, in order to recover the geo-reference information of each pixel in the newly transformed T3. Speckle effects are inherent noises resulting from the coherent interference of the waves that have been reflected from elementary scatter [18,19]. In order to achieve optimal speckle-reduction in SAR image, filter with window size 7 × 7 were used [20].

The Freeman-Durden decomposition is a method for fitting a physically based, three-component scattering mechanism model to polarimetric SAR observations. The three-component scattering mechanism includes surface, double-bounce and volume scattering mechanisms [19]. This approach can be used to determine the dominant scattering mechanisms and to facilitate identifying the current state of the surface cover. In addition, the three-component scattering may

provide features for distinguishing between different surface cover types.

The thematic maps were digitized and converted into GIS format for spatial analysis. The digital image processing was carried out using ENVI 5.1 package. In addition, the GIS analysis was carried out using ArcGIS 10.2 package. The sequential process of obtaining the final lithological map could be summarized as follows:

a) Data fusion of the above processed polarimetric data with the optical PCA data,
b) Visual characterization of the lithological units and rock types,
c) Classification of the data fused to categorize the lithological units and different rock types,
d) Conversion of the classified raster image into vector GIS data format,
e) Further improvements of the border of the lithological units rock types (vector GIS data layer) using manual adjustments and digitizing based on the pattern and harmony of the rock units,
f) Validation of the result in step e with the thematic geological maps and results from field survey for ensuring high level of certainty,
g) Last, the final lithological map is created with proper layout and symbology.

4. RESULTS AND DISCUSSION

The geological map of the Central Desert of Sinai has been categorized the outcrops of Nekhel area into three main components [21], a) Wadi deposits, b) Alluvial deposits, and 3) Egma formation. Egma formation consists of chalky limestone with flint bands and nodules at base and thin successive chert bands at top (Fig. 2). This geological map of Nekhel area is, however, at large scale (1:250 000) is not capable to present details of each sedimentary class or/and lithological unit. The boundaries between these classes are not sharp in reality and not located correctly from a geographical point of view which may lead to misinterpreting the depositional history. Therefore, there is a need for more accurate mapping of the surface sediments that capable to categorize and differentiate between the sedimentological classes in Nekhel area. This is based on optical and radar data that help better understanding of the depositional history of the Nekhel area and might provide an economic value of such deposits.

Landsat 8 band combination 7-3-2 (Fig. 3a) and ASTER band combination 7-3-1 which used as equivalent to Landsat ETM 7-4-2 image [22], (Fig. 3b). These false color composite images were helpful in defining the boundaries of the Wadi deposits in the study area. 6 Principal Component Analysis (PCAs) bands were obtained from the 6 Landsat 8 channels (i.e. VNIR, SWIR) and 9 PCAs bands were also obtained from the 9 ASTER channels (i.e. VNIR, SWIR). Basically, the statistical analysis of the PCA always concentrates the information ascending from the first PCA downwards. To ensure the high applicability of the PCA composite in characterization and differentiation of rock types, all PCAs eigenvectors were analyzed to the corresponding rock type. This analysis has resulted in those 3 PCAs (PC6, PC2 and PC1) out of the 6 generated from Landsat 8 images, and 3 PCAs (PC4, PC2 and PC1) out of the 9 generated from ASTER images were found to be more appropriate and efficient (Fig. 3c & Fig. 3d). The best RGB color composites for visualizing the lithological discrimination using these PCAs are (RGB: PC6, PC2 and PC1) for better characterization and discriminate of the Wadi deposits in white and whitish blue.

Also optical data including Landsat 8 and ASTER could be functioned in band math such as band-ratio that enable for improving the discrimination of objects. Color composite combination of the band math ratio is also an effective tool to emphasizing spectral characteristics of certain rocks and minerals and improve lithological mapping [23,24]. The color composite of the band ratio (6/3, 1/3, 9/5) is very efficient for mapping the lithology in Wadi Kid in Sinai, Egypt [25] (Fig. 4a).

Single ratio of Landsat 8 data (6/2, 6/7, 6/5 * 4/5) (Fig. 4b) enabled to discriminate acidic, basic and intermediate metavolcanics as well as Hammamat sediments at Abu Marawat-Semna area, Central Eastern Desert, Egypt. However, single ASTER data in band-ratio (4/7, 4/10, 4/11) (Fig. 4c) that integrates SWIR and TIR able to characterize and map the lithological units (e.g. Fawakhir area, Central Eastern Desert, Egypt). This shows high performance in the mapping and differentiation of the lithological units. Indeed, all the band ratios show a better discrimination of the different rock units in the study area. The ratio composite (4/7, 4/10, 4/11) gives a slightly better contrast where Alluvial deposits well separated from adjacent rocks by dark red color [26].

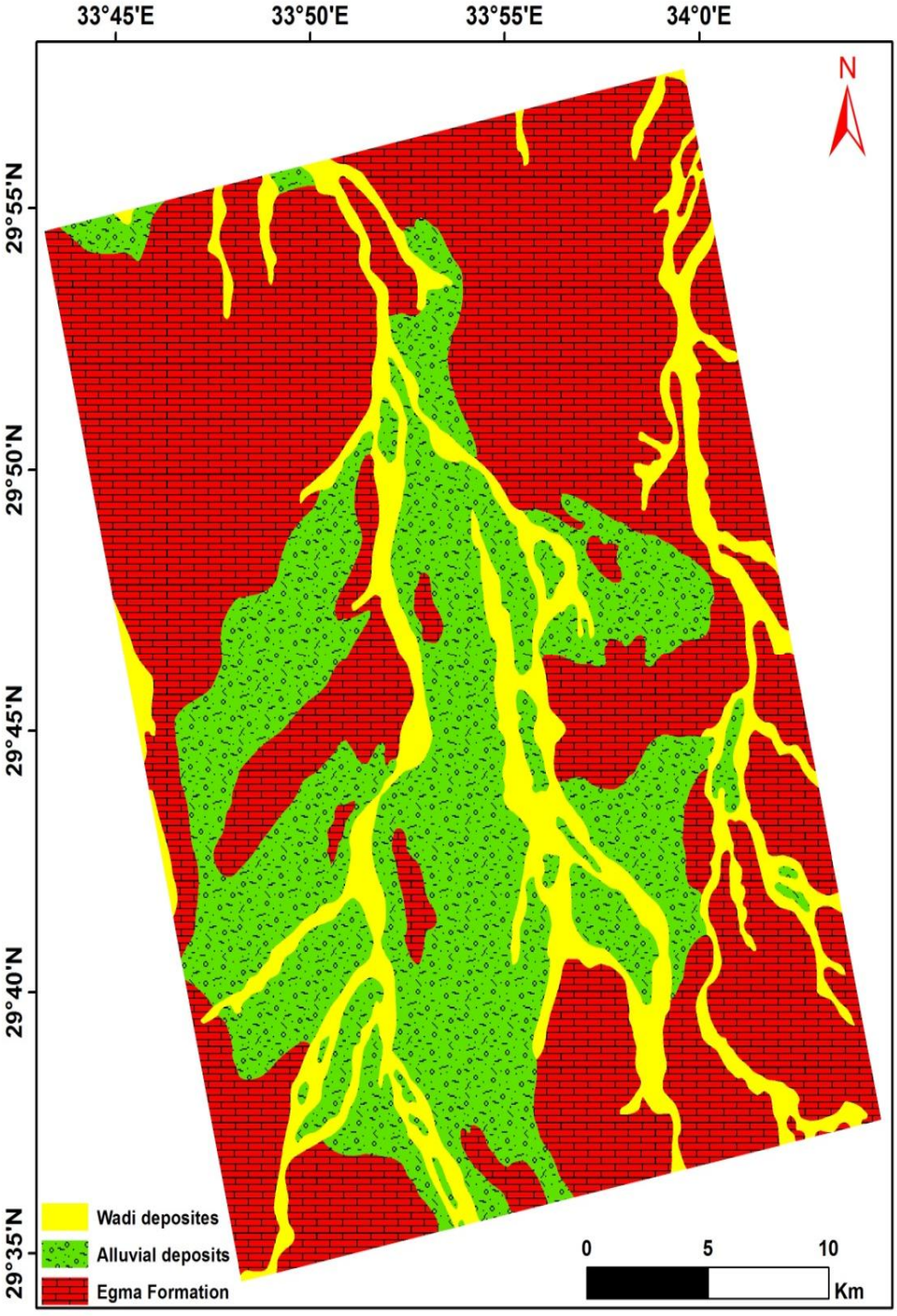

Fig. 2. The geological map of Nekhel area, Sinai, Egypt [21]

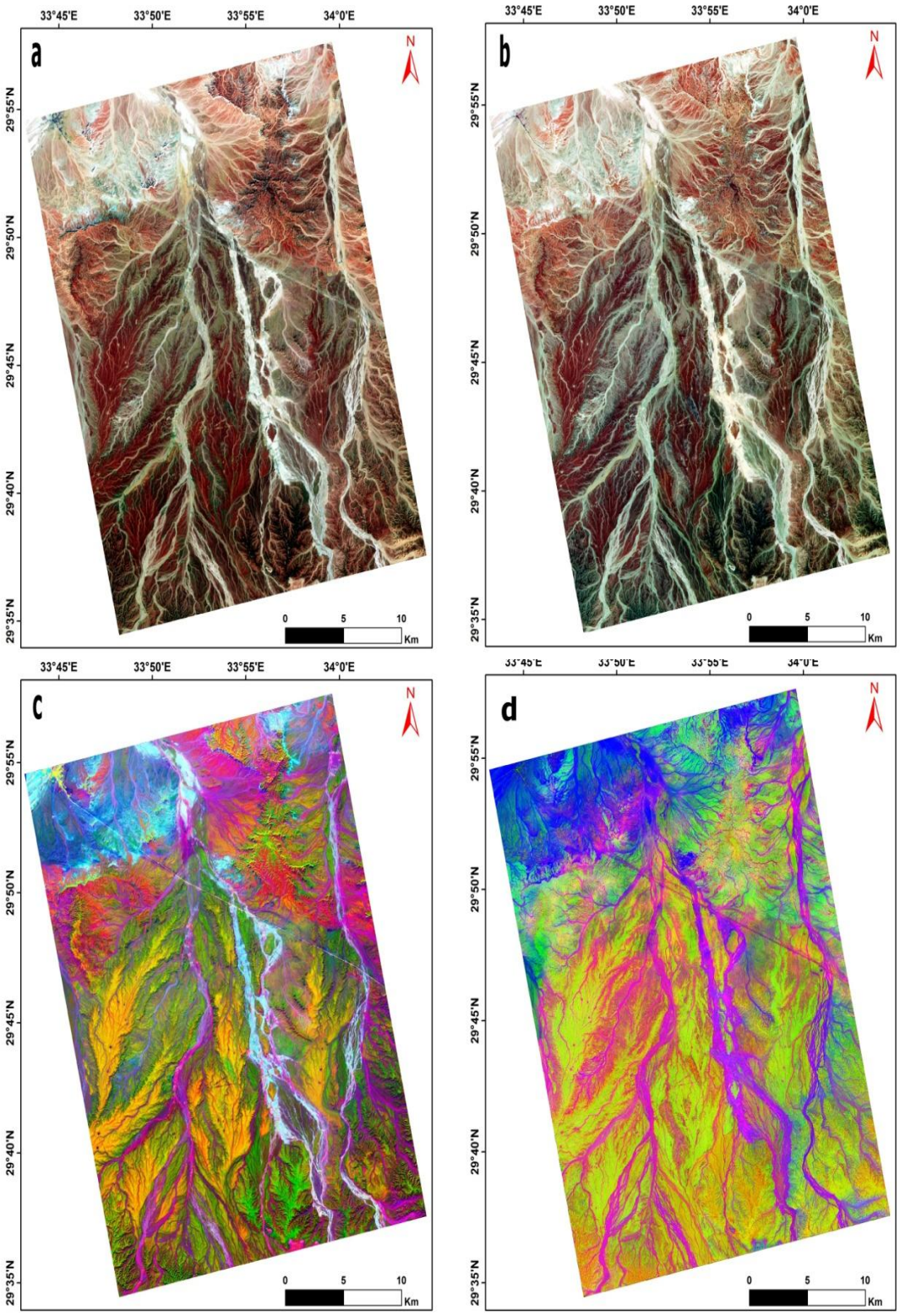

Fig. 3. (a) Landsat 8 false color composite of 7-3-2 (b) ASTER false color composite of 7-3-1 (c) PC6, PC2, PC1 (d) PC4, PC2, PC1

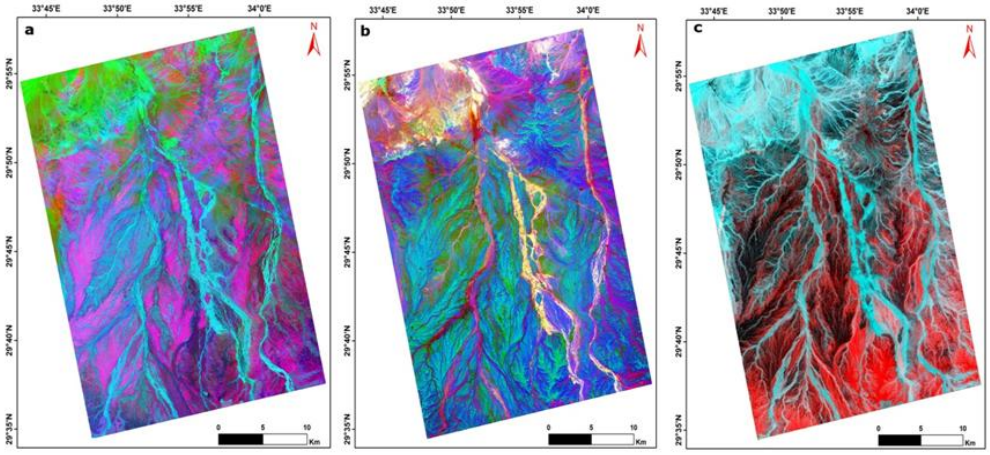

Fig. 4. Band ratios (a) 6/3-1/3-9/5 [25]; (b) 6/2-6/7-6/5*4/5; (c) 4/7-4/10-4/11 [26]

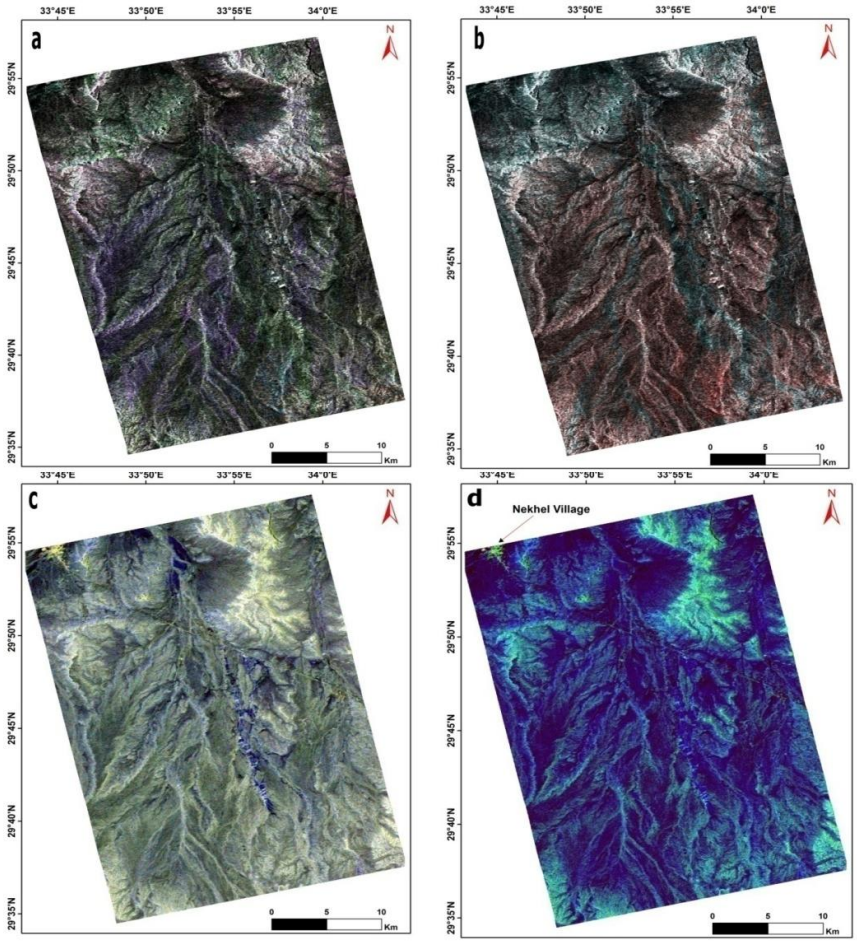

Fig. 5. (a) Landsat 8 band ratio (6/2-6/7-6/5*4/5) with RADARSAT-2 band (T33) fused image (b) ASTER band ratio (6/3, 1/3, 9/5) with RADARSAT-2 band (T33) fused image (c) The Pauli RGB image (d) Freeman-Durden decomposition image

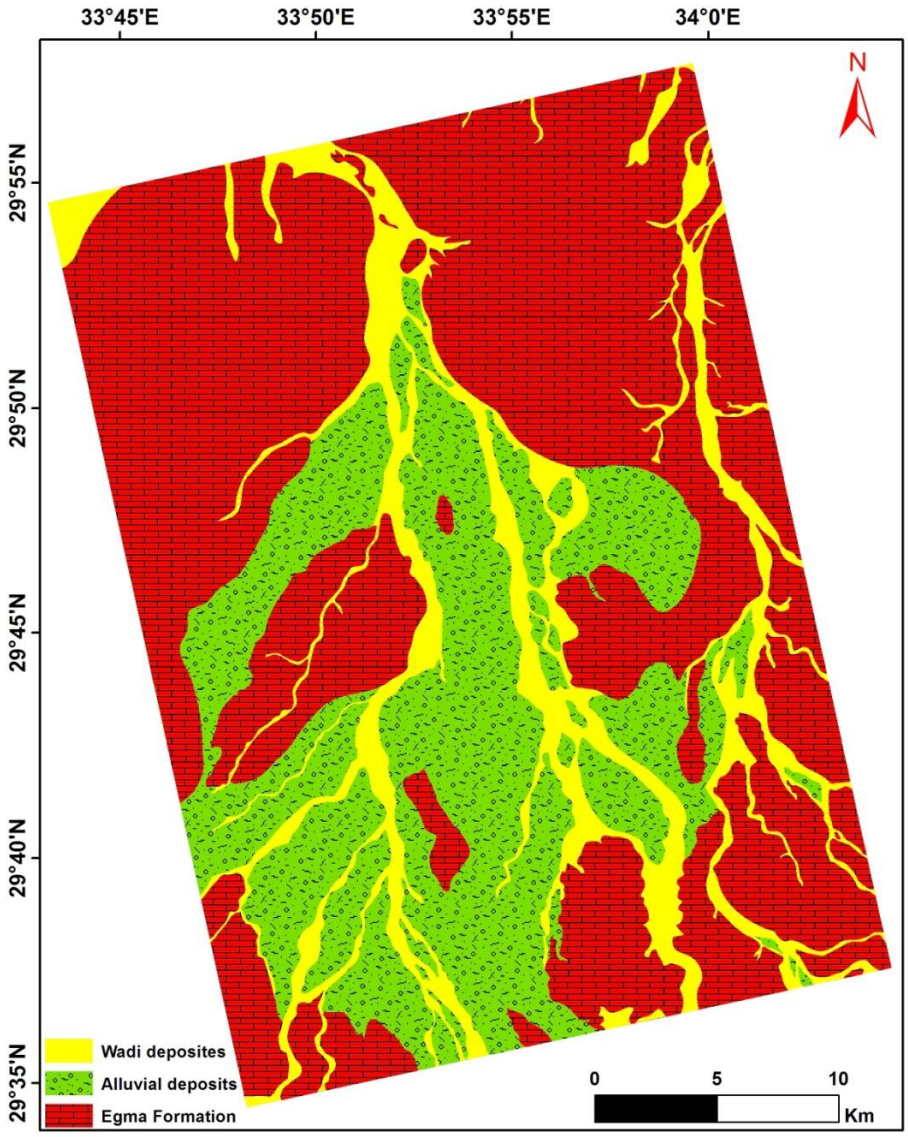

Fig. 6. Final lithological map of the Nekhel area, Sinai Penensula as resulted from the integration of optical and radar remote sensing data

When polarimetric radar data are analyzed, a number of parameters that have a useful physical interpretation can be computed. T3 coherency and C3 covariance matrix are fundamental matrices, from which other decomposition parameters can be derived [19]. Among all the parameters in T3, the diagonal elements T11 (|HH+VV|), T22 (|HH-VV|), and T33 (|HV|) contain the most useful polarimetric information. The widely used Pauli decomposition is based on the T3 matrix. Each of the parameters has clear physical meaning: T11 represents single (odd) bounce scattering, T22 indicates double bounce scattering, and T33 is associated with volume scattering [19]. The Pauli RGB (Fig. 5c) gives information about the dominant scattering mechanism along the study area, where the green color means volume scattering, the red means double scattering, and blue means surface scattering. The black color in Pauli RGB image means Bragg scattering or the signals were totally attenuated.

Landsat 8 band ratio (6/2-6/7-6/5*4/5) with RADARSAT-2 band (T33) (Fig. 5a) and ASTER band ratio (6/3, 1/3, 9/5) with RADARSAT-2 band

(T33) (Fig. 5b) fused images have slightly improved the ability to discriminate between different rock types on the basis of their spectral and back-scattering characteristics. For example, the dendritic nature of the drainage system is obvious and well-illustrated. Egma formation is defined by white to pale green colors in Landsat 8 fused image.

The Freeman-Durden incoherent target decomposition image (Fig. 5d) reveal the urban areas which appear as green and Egma formation is green due to a high volume scattering. The Wadi deposits and the alluvial deposits appear in light blue pattern due to a high surface scattering because of smoother surfaces. The road and power line appear as bright lines and red spots due to double-bounce scattering. Information obtained from these analyses was organized into a database and analyzed using ArcGIS 10 software that has been also used to generate the final lithological map of the study area (Fig. 6).

5. CONCLUSION

In conclusion in open barren dry land such as Sinai Peninsula, the conventional methods of geological mapping at large scales always fail to accurately differentiate between the sedimentological classes. Optical remote sensing data could be to some extent to identify the boundaries between the different lithological units with some limitations. Therefore, this research explored the potentiality of integrating polarimetric SAR that is working on the roughness of the lithological units, as well as the composition with the optical data. The approach was able to maximize the value of combination between the two data sensors to improve the characterization and classification of the lithological units and sedimentological units. Data fusion of optical (ASTER and Landsat8) and radar data found to be an efficient approach of identifying different lithological units on the basis of their spectral characteristics and surface roughness, particularly in arid regions such as Sinai Peninsula. Landsat 8 and ASTER-RADARSAT-2 data fusion illustrates the usefulness of such methodology for mapping different lithological units. It is recommended that further research on remote predictive mapping of the various rock units with detailed ground geological data to improve the validation process and generically stabilize this model for lithology mapping.

COMPETING INTERESTS

Authors have declared that no competing interests exist.

REFERENCES

1. Abrahams AD, Parsons AJ, (Eds.). Geomorphology of desert environments. London: Chapman Hall. 1994;674.
2. Glennie KW. Desert sedimentary environments. Amsterdam: Elsevier. 1970; 221.
3. Dobson MC, Pierce LE, Ulaby FT. The role of frequency and polarization interrain classification using SAR data. IEEE Transactions on Geoscience and Remote Sensing. 1997;35(4):1621–1623.
4. Boerner W, Mott H, Luneburg E, Livingstone C, Brisco B, Brown R, Paterson S. Polarimetry in radar remote sensing: Basic and applied concepts. In F.Henderson, & A. Lewis (Eds.), (3rd Edition).Manual of Remote Sensing. 1998; 2:271–357.
5. Van Zyl JJ. Unsupervised classification of scattering behavior using radar polarimetrydata. IEEE Transactions on Geoscience and Remote Sensing. 1989; 27(1):36–45.
6. Van Zyl JJ, Zebker HA. Imaging radar polarimetry. In J.A. Kong (Ed.), Progressin Electromagnetics Research. Pier. 1990;3: 277–370.
7. Zebker HA, van Zyl JJ. Imaging radar polarimetry: A review. Proceeding of the IEEE. 1991;79(11):1583–1606.
8. Canadian Space Agency, Departmental Performance Report (2007-2008).
9. Vincent RK, Thomson F, Watson K. Recognition of exposed quartz sand and sandstone bytwo-channel infrared imagery. J. Geophys. Res. 1972;77:2473–2477.
10. Goetz FH, Billingsley FC, Gillespie AR, Abrams MJ, Squires RL, Shoemaker EM, Lucchitta I, Elston DP. Application of ERTS images and image processing to regional problems and geological mapping in northern Arizona, JPL Technical Report. 1975;32–1597.
11. Holben BN, Justice CO. An examination of spectral band ratioing to reduce the topographic effect on remotely sensed data. Int. J. Remote Sensing. 1981;2(2): 115–133.

12. Chavez Jr. PS, Sides SC, Anderson JA. Comparison of threedifferent methods to merge multiresolution and multispectral data; Landsat TM and SPOT panchromatic. Photogrammetric Engineering and Remote Sensing. 1991; 57:295–303.
13. Jensen JR. Introductory digital image processing. Prentice HallSeries in Geographic Information Science. 1996; 318.
14. Bretschneider T, Kao O. Image fusion in remote sensing. In: Proceedings of the 1st Online Symposium of Electronic Engineers. 2000;CD-ROM.
15. Hugenholtz C, Van der Sanden J. Polarimetric SAR for geomorphic mapping inthe intertidal zone, Minas Basin, Bay of Fundy, Nova Scotia. 24 (Preprint Canada Centrefor Remote Sensing); 2001.
16. Boerner WM. Introduction to synthetic aperture radar (SAR) polarimetry. New York: Wexford College (Ch. 1); 2007.
17. ESA..PolSARpro_Data Format; 2008. Available:http://earth.eo.esa.int/polsarpro/Manuals/
18. Lee JS, Grunes MR. Classification of Multi-Look Polarimetric SAR DataBased on Complex Wishart Distribution. Intern. J. Remote Sensing. 1994;15(11):2299-2311.
19. Lee JS, Pottier E. Polarimetric Radar Imaging: from Basics to Applications. Boca Raton, United States: Taylor & Francis Group. 2009;438.
20. Lee JS. Refined filtering of image noise using local statistics. Computer Graphicsand Image Processing. 1981; 15(4):380–389.
21. EGSMA. Geological map of Sinai, Arab Republic of Egypt "Sheet No. 2 with scale 1:250,000; 1994.
22. Abdeen MM, Allison TK, Abdelsalam MG, Stern RJ. Application of ASTER band-ratio images for geological mapping in arid regions; the Neoproterozoic Allaqi Suture, Egypt. Abstract with Program Geol. Soc. America. 2001;3(3):289.
23. Okada K, Ishii M. Mineral and lithological mapping using thermal infrared remotely sensed data from ASTER simulator. Int. Geosci. and Remote Sensing Symposium "Better Understanding of Earth Environment". 1993;93:126–128.
24. Hewson R, Cudahy T, Huntington J. Geologic and alteration mapping at Mt Fitton, South Australia, using ASTER satellite-borne data. Geoscience and Remote Sensing Symposium. 2001;2:724-726.
25. Gad S, Raef A. Factor analysis approach for composited ASTER band ratios and wavelet transform pixel-level image fusion: Lithological mapping of the Neoproterozoic Wadi Kid area, Sinai, Egypt. Int. J. Remote Sens. 2012;33(5):1488e1506.
26. Mohy H, Abou El-Magd I, Basta F. Newly improved band ratio of ASTER data for Lithological Mapping of the Fawakhir Area, Central Eastern Desert, Egypt. Journal of the Indian Society of Remote Sensing. 2016;44(5):735-746.

Peer-review history:
The peer review history for this paper can be accessed here:
http://www.sciencedomain.org/review-history/24532